

Supporting Information

In Situ Investigation of Detoxification and Metabolic Effects of Polyfluoroalkyl Substances on Metal-Organic Frameworks Combined with Cell-Cultured Microfluidics

Ning Xu, Haifeng Lin, Qiuling Du, Shujun Dong, Jie Cheng, Peilong Wang*, and Jin-Ming Lin*

Table of Contents

1. Chemicals and materials	1
2. Manufacture the microchip	1
3. Adsorption characterization	4
4. Sorption kinetic	7
5. Adsorption isotherms of FTOHs in BUT-16	7
6. Effects of static and fluidic adsorption on the cell proliferative activity	8
7. Online SPE- MS/MS condition	9
8. Qualitative and quantitative analysis of target compounds	10
9. Inflammatory cytokine assay	13
Table S1. Parameters of the pseudo-first-order and the pseudo-second order model for the adsorption of FTOHs on BUT-16.	14
Table S2. Performance of two adsorption systems.	14
Table S3. Langmuir and Freundlich constants for the sorption of FTOHs using BUT-16.	14
Table S4. The LOD, calibration, linear ranges and RSD of target compounds.	15
Table S5. A list of 65 metabolites identified with database.	16
References	17

1. Chemicals and materials.

The 6:2 FTOH and 8:2 FTOH were purchased from Sigma-Aldrich (Saint Louis, USA), 10:2 FTOH was bought from J&K Scientific (Shanghai, China), FTCAs (6:2, 8:2 and 10:2) and isotopically labeled 1,2-¹³C₂-FTCAs (6:2, 8:2 and 10:2) were obtained from Wellington Laboratories (Ontario, Canada). LC-MS grade water, methanol, formic acid, isopropanol and ammonium formate were from Fisher Scientific (Fairlawn, NJ).

2. Manufacture the microchip

The photo mask was designed twelve cell culture channels to satisfy the experimental variables and make high throughput detection of metabolites. This microchip was fabricated by soft lithography and replica molding techniques¹. An SU-8 2050 negative photoresist (Microchem, USA) was spin-coated on a cleaned silicon wafer. After soft bake in the oven and cooling down to room temperature, the wafer was covered with the photo mask and exposed to UV light for 2 min. The silicon mold was developed by developing solution (Microchem, USA). A 10:1 weight mixture of PDMS prepolymer and curing agent (Sylgard184, Dow corning) was then poured onto the silicon mold and baked in the oven at 65 °C for 2 h. Then the PDMS was peeled from the wafer mold, and connection holes were punched before the PDMS replica was irreversibly sealed with glass slides by oxygen plasma treatment (PDC-32G, Harrick Plasma, Ithaca, NY).

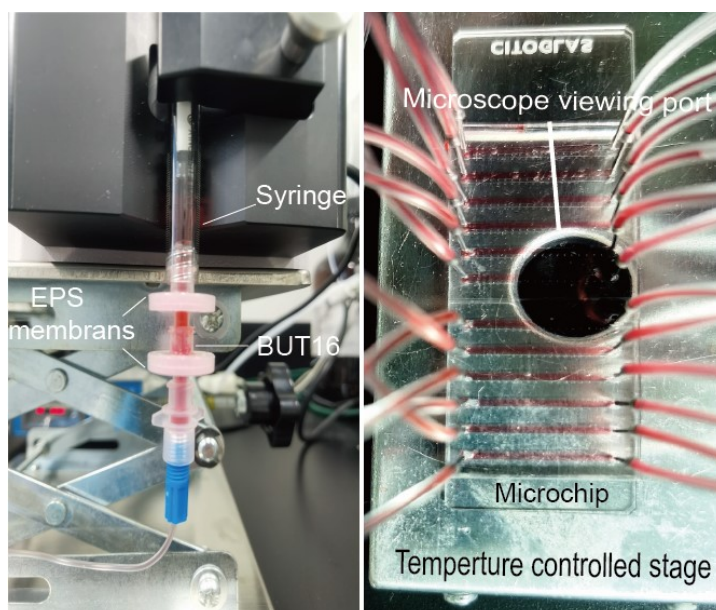


Figure S1. Photograph of the FTOHs filter (left) and microfluidic device (right)

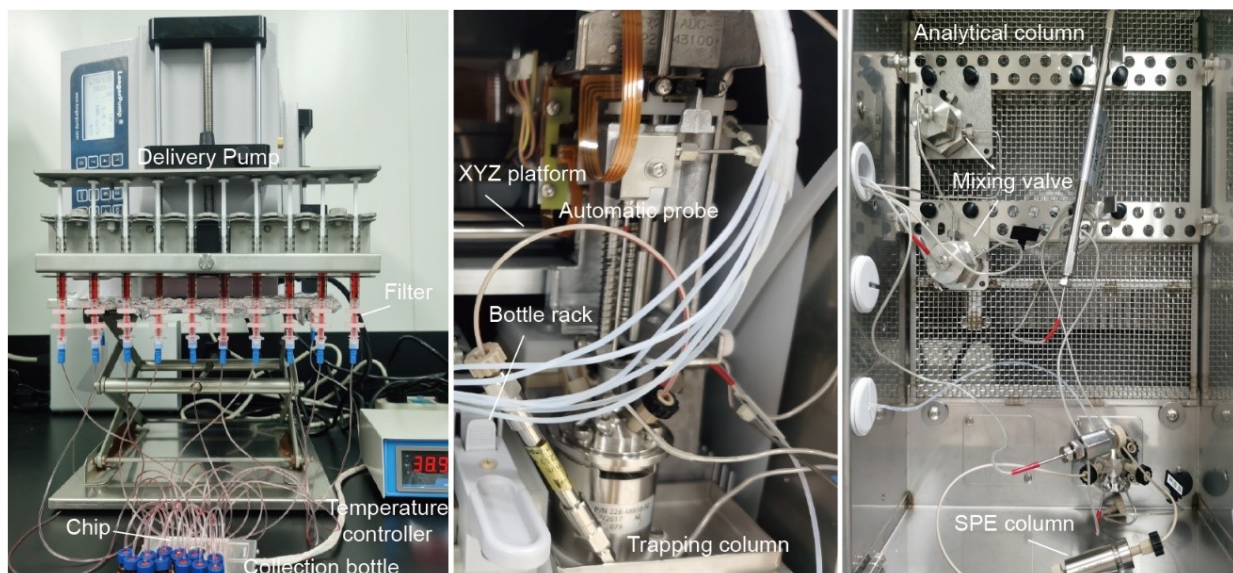


Figure S2. Photograph of the experimental instrument.

3. Adsorption characterization

For comparison, other MOF materials were tested for adsorption of FTOHs, including BUT-17², UIO-66³, UIO-66-NH₂⁴, and MIL-101(Fe)⁵. The adsorption efficiency reaches more than 60%, while BUT-16 has a better adsorption capacity for FTOH under the same conditions, and the adsorption efficiency can be reached as high as 100%. At the same time, we used the CCK-8 assay (Dojindo Laboratories, Japan) to test the cytotoxicity of different materials, data indicated that toxic potency of BUT-16 to cells was negligible. The above results show that BUT-16 has high adsorption efficiency and safety. In order to clarify the adsorption effect of BUT16, fourier transform infrared spectroscopy (FT-IR) and powder X-ray diffraction were used to analyze the adsorption of BUT-16. After adsorption of 500 mg/mL FTOHs, compared with BUT-16 before adsorption, the FT-IR spectrum showed new peaks around 1200-1350 cm⁻¹, which were consistent with the characteristic peaks of -CF₂ and -CF₃ reported in literature⁶. Moreover, the PXRD pattern of the synthesized BUT-16 is almost identical to the simulated XRD pattern, indicating successful synthesis and good crystallization. Adsorbed BUT-16 also had the same pattern, indicating that the structure is maintained before and after adsorption. In addition, we observed the adsorption of 100 mg/L FTOH by X-ray photoelectron spectroscopy (XPS), the F element appeared in the XPS spectrum.

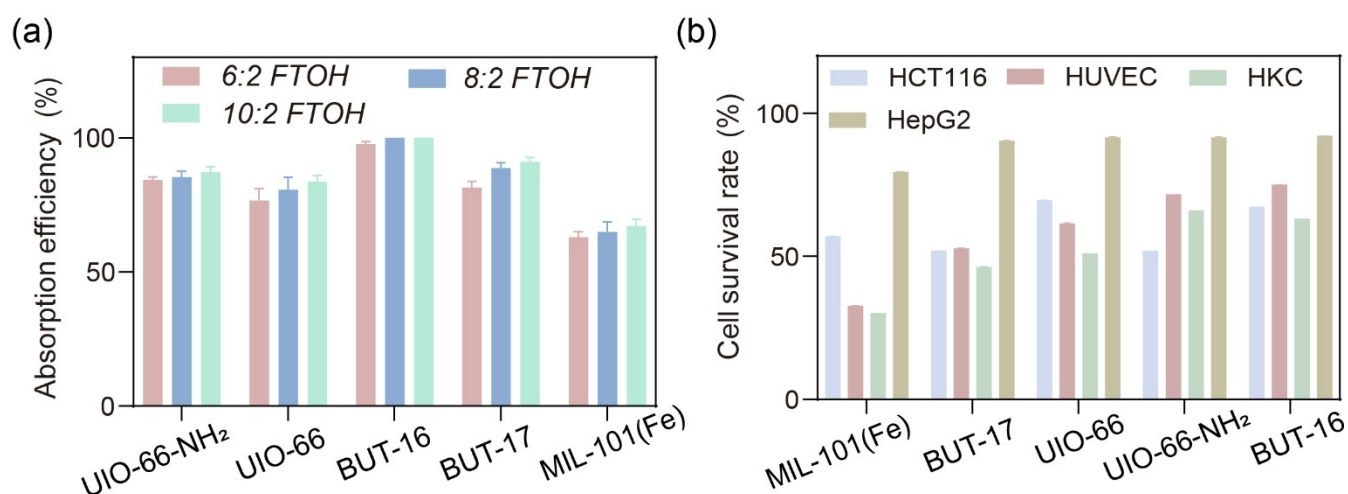


Figure S3. (a) Adsorption efficiency of FTOHs in aqueous solution with 3mg/L BUT-16 and other adsorbents. (b) Survival rate of four types of cells in cell culture medium with 3mg/L BUT-16 and other adsorbents. Data are presented as mean \pm SD at least three replicate experiments

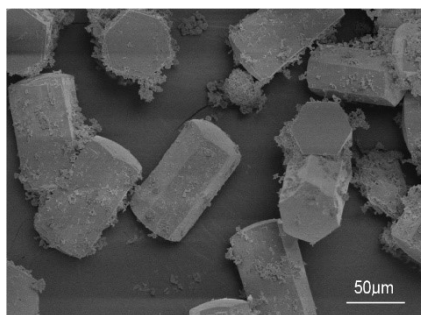


Figure S4. The SEM image of BUT-16

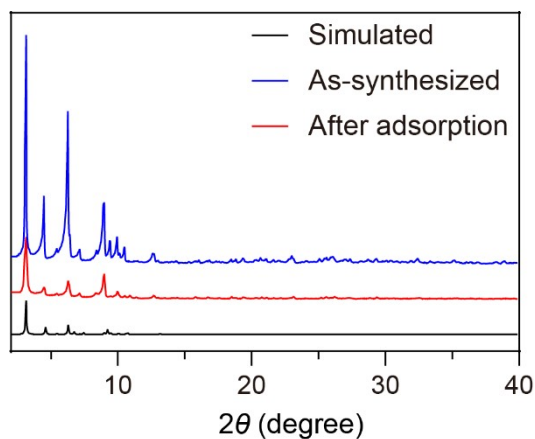


Figure S5. XRD patterns of BUT-16 before and after adsorption

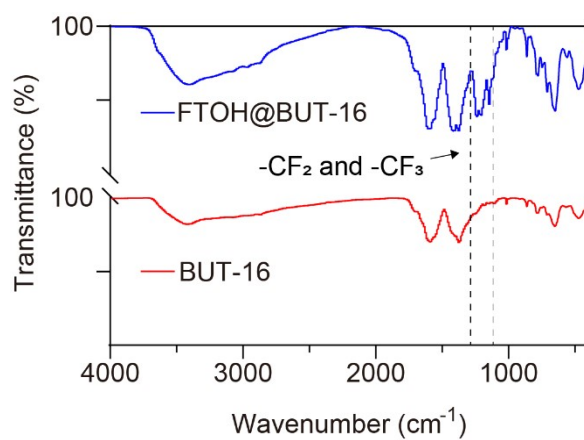


Figure S6. FT-IR spectra of BUT-16 before and after adsorption.

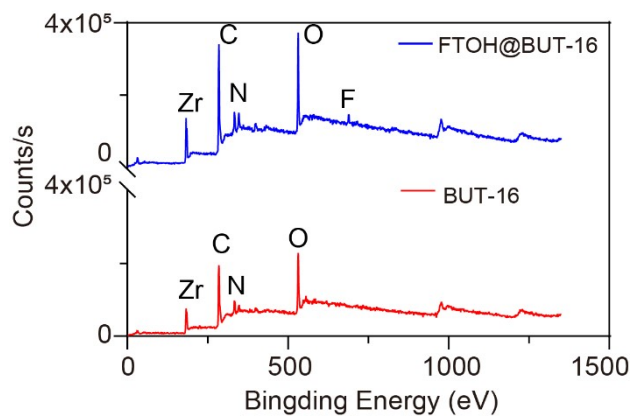


Figure S7. XPS spectra of BUT-16 before and after adsorption.

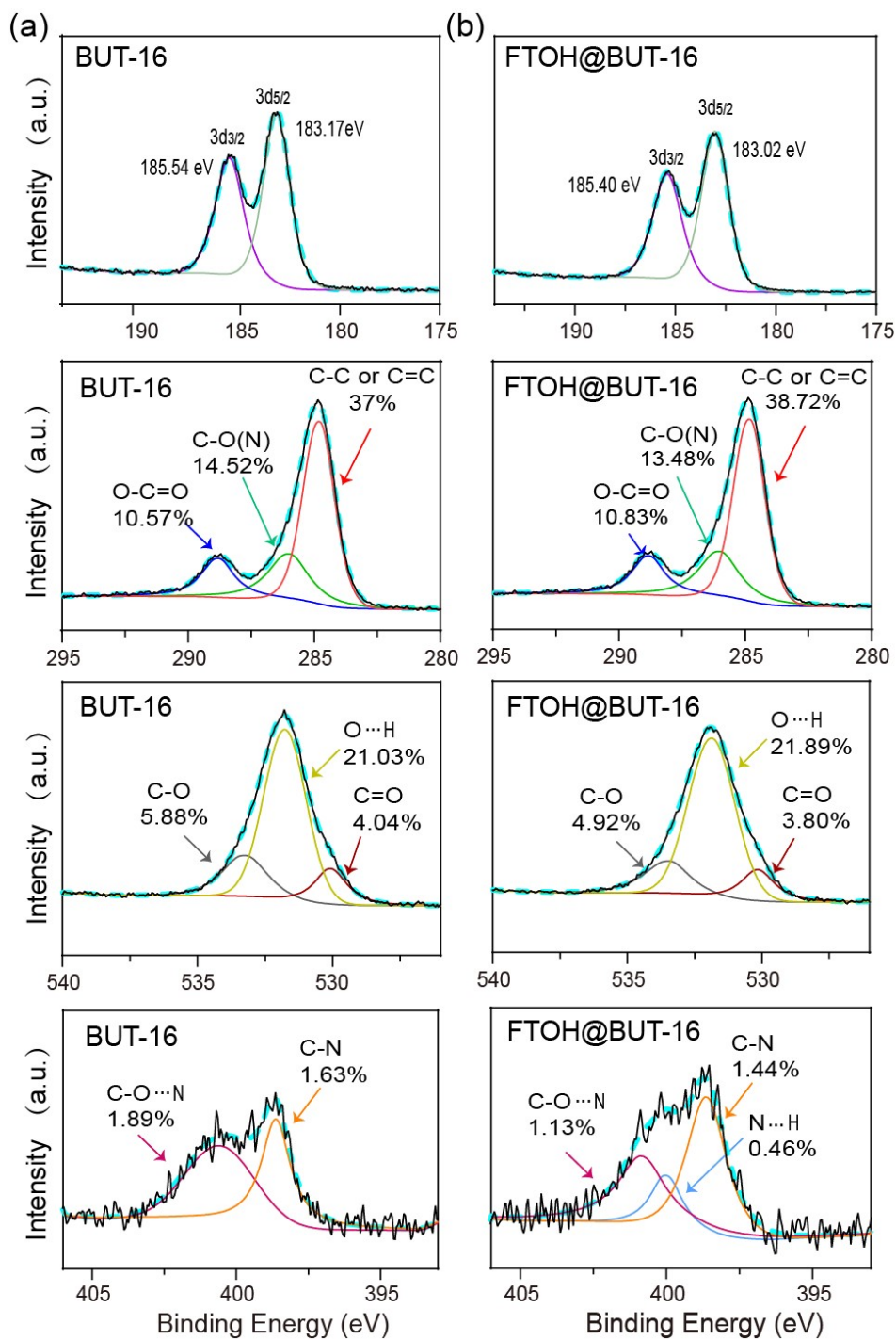


Figure S8. High-resolution Zr 3d_{3/2} and Zr 3d_{5/2}, C1s, O1s, N1s XPS spectra of (a) BUT-16 and (b) FTOH@BUT-16.

4. Sorption kinetic

FTOHs adsorption efficiency experiments were performed. Firstly, the primary stock solution was diluted to 500 mg/L to obtain an aqueous solution of FTOHs. fluidic adsorption was then performed through a filter loaded with 3 mg/mL BUT-16 at a certain flow rate. While in static adsorption, the glass tube was filled with 4 mL of FTOHs aqueous solution and 12 mg of slightly grinding BUT-16, and the glass tube was shaken on a shaker. Finally, samples were taken at different times and the concentration of residual FTOHs in the supernatant was detected by ultraperformance liquid chromatography coupled tandem mass spectrometry (UPLC–MS/MS).

The sorption kinetic curves are fitted with pseudo-first-order equation (1) and pseudo-second-order equation (2) as followed:

$$\ln(Q_e - Q_t) = \ln Q_e - k_1 t \quad (1)$$

$$\frac{t}{Q_t} = \frac{1}{k_2 Q_e^2} + \frac{t}{Q_e} \quad (2)$$

In the equation 1 and 2, t (min) is the adsorption time, Q_t (mg/g) and Q_e (mg/g) is the adsorption capacity at the different time and the equilibrium adsorption capacity for BUT-16, respectively. k_1 (min^{-1}) and k_2 ($\text{g min}^{-1} \text{mg}^{-1}$) is the constant of pseudo-first-order equation and pseudo-second-order equation, respectively.

5. Adsorption isotherms of FTOHs in BUT-16

To obtain the adsorption isotherms, a series of FTOHs initial solutions with gradient concentrations changed from 1 to 12000ppm were formulated with 3 mg/mL BUT-16. The data of the adsorption isotherms were fitted with Langmuir (1) and Freundlich (2) models.

$$\frac{C_e}{Q_e} = \frac{1}{k_L Q_m} + \frac{C_e}{Q_m} \quad (1)$$

$$\ln(Q_e) = \frac{1}{n} \ln C_e + \ln K_F \quad (2)$$

Q_e is the adsorbed amount at equilibrium, C_e (mg/L) is equilibrium concentration, and K_L (L/mg) and Q_m (mg/g) are the Langmuir constant and Langmuir equilibrium adsorption capacity, respectively. K_F ($[\text{L/mg}]^{1/n} \text{mg/g}$) and n are the Freundlich parameters, related to adsorption capacity and intensity, respectively.

6. Effects of static and fluidic adsorption on the cell proliferative activity

In order to illustrate the necessary of fluidic adsorption, we explored the effect of cytotoxicity. Firstly, the FTOHs were spiked at 5, 10, 50, 100, 200, 300, 400 and 500mg/L each to DMEM/F12 with 5% FBS and 1% antibiotics solution. Next, this medium 500mg/L FTOHs of was static or fluidic adsorbed by BUT-16, and the cells were incubated for 24 h. Finally, the effect of cell viability was assessed by CCK-8 assay.

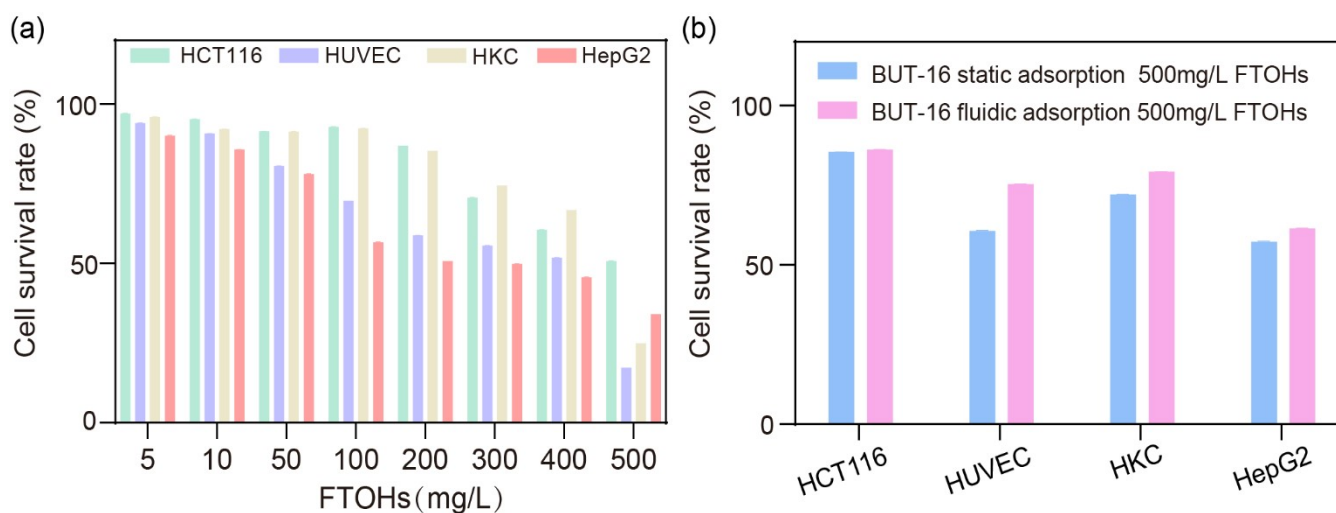


Figure S9. (a) Survival rate of four types of cells in different concentration of FTOHs. (b) Survival rate of four types of cells in BUT-16 static and fluidic adsorption 500mg/L FTOHs. Data are presented as mean \pm SD at least three replicate experiments.

7. Online SPE- MS/MS condition

SPE column was coupled with analytical column in the UPLC device, an extensive optimization of the selective online extraction conditions was conducted. For analysis of FTOHs and its metabolites, the online SPE was used Shim-pack MAYI-ODS column (4.6mm i.d.×10mm, particle diameter 50µm, Shimadzu) and separation used a CAPCELL PAK AQ C18 column (2.0mm i.d.×150 mm, particle diameter 3µm, Osaka Soda). The washing mobile phase containing 10% acetonitrile in water was held at 1mL/min for the first 1 min for eliminating salt and protein, and then quickly decreased to 0.3mL/min over 2 s and kept for 7 min. Meanwhile the elution mobile phase consisted of (A) 10mM ammonium acetate in water and (B) 8:2 methanol: acetonitrile and used the following gradient program: 0-1min 60% B, 2-5.9 min 100% B, 6-10min 60% B. It maintains at 0.35mL/min. One minute later, the valve was switched from the precolumn to the separation channel. The entire analysis cycle was estimated to be 10 min for each sample from injection to column washing. The trapping column was used a C18 column (2.1mm i.d.×50 mm, particle diameter 3µm, Shimadzu)

For analysis of small molecules such as amino acids, nucleic and sugar, the online SPE was used CAPCELL PAK MF SCX SG80 column (2.0mm i.d.×100mm, particle diameter 5µm, Osaka Soda) and separation used CAPCELL PAK CR 1:4 column (2.0mm i.d.×150 mm, particle diameter 5µm, Osaka Soda). The washing mobile phase containing 50% acetonitrile in water was held at 0.7mL/min for the first 0.5 min for eliminating salt and protein, and then quickly decreased to 0.3mL/min over 2 s and kept for 12.5 min. Meanwhile the elution mobile phase consisted of (A) 0.1% formic acid in water and (B) 0.1% formic acid in acetonitrile and used the following gradient program: 0-2min 0% B, 2-5min 25% B, 5-9min 35% B, 9-12min 95% B, 12-13min 95%, 13-18min 0% B. It maintains at 0.35mL/min. 0.5 minute later, the valve was switched from the precolumn to the separation channel. The entire analysis cycle was estimated to be 18 min for each sample from injection to column washing.

The mass spectrometric conditions were optimized as follows: interface temperature: 300 °C; heating block temperature: 250 °C; DL temperature: 150 °C; spray voltage: 4.00 kV; nebulizer gas (N₂) flow rate: 3L/min; heating gas (N₂) and drying gas (N₂) flow rate: 10 L/min, respectively.

8. Qualitative and quantitative analysis of target compounds

A working standard solution was prepared from each stock solution by dilution with culture medium containing DMEM/F12, 5% FBS and 1% antibiotics solution, yielding concentrations of 6:2, 8:2 and 10:2 FTOH ranging from 1 to 50 mg/L (1, 5, 10, 20, and 50 mg/L), concentration of 6:2, 8:2, 10:2 FTCA ranging from 156.25 to 10000 ng/L (156.25, 312.5, 625, 1250, 2500, 5000, 10000ng/L). The solution of an isotopically labelled internal standard, 1,2-¹³C₂-FTCA was prepared using the same procedure and added to working standard solution at a concentration of 10000ng/L. Calibration curve was constructed by plotting each target compound concentration against the corresponding peak area and fitting the data using linear regression.

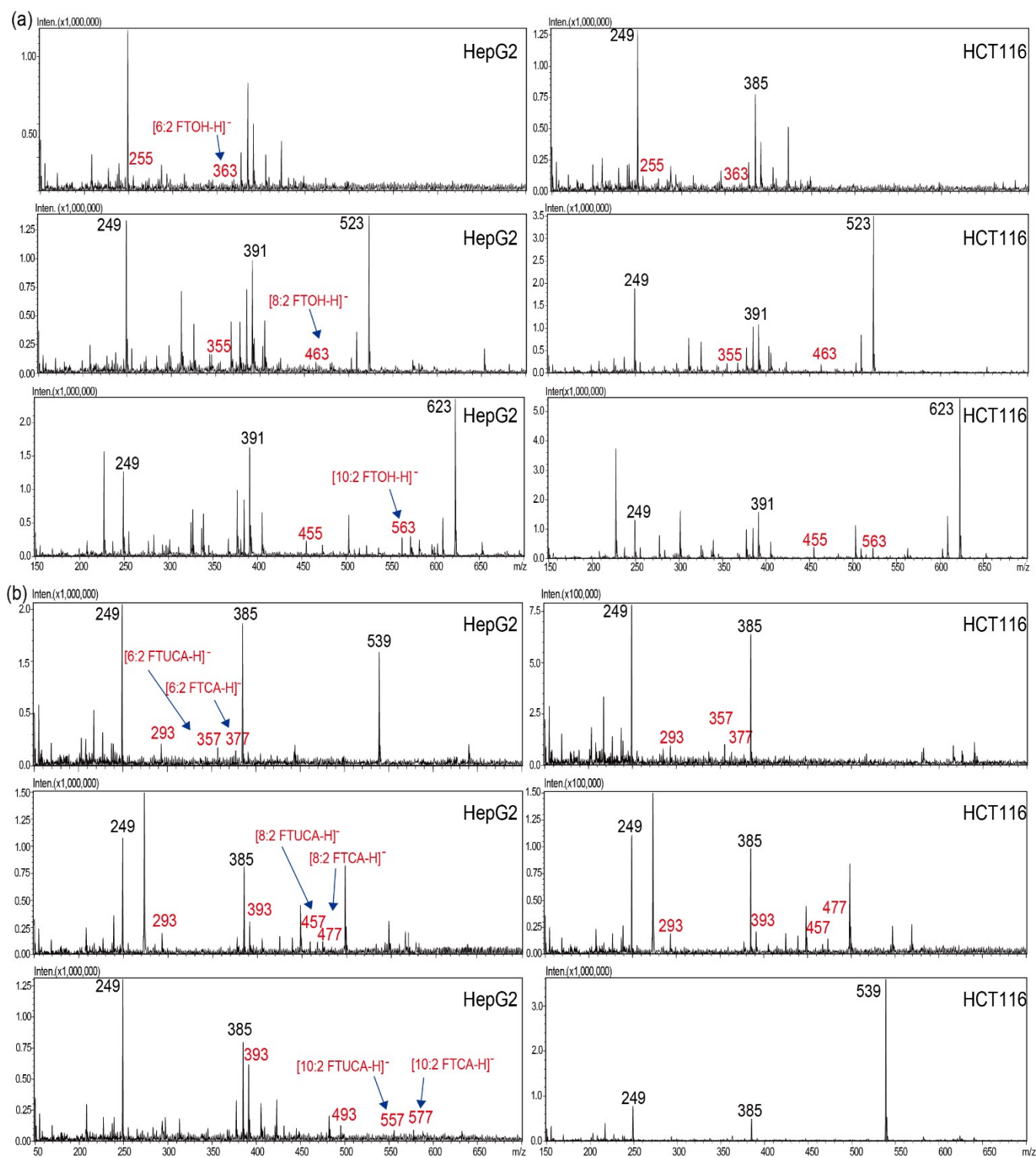


Figure S10. Monitoring of FTOHs metabolites. Mass spectra of (a) 6:2, 8:2, 10:2 FTOH and (b) 6:2 FTCA, 6:2 FTUCA, 8:2 FTCA, 8:2 FTUCA, 10:2 FTCA, 10:2 FTUCA of the experiment implemented by HepG2 cells and HCT116 cells being incubated with 6:2, 8:2, 10:2 FTOH.

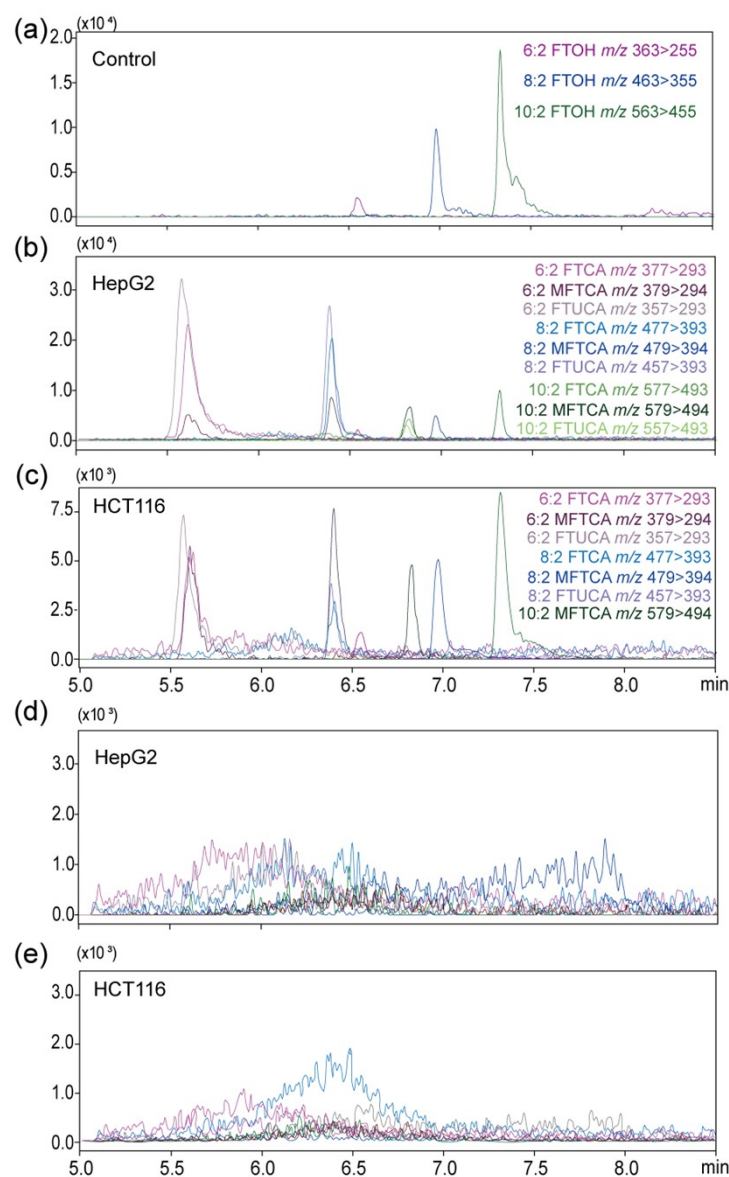


Figure S11. Ion chromatographic peaks of metabolic compound 6:2 FTCA, 6:2 FTUCA, 8:2 FTCA, 8:2 FTUCA, 10:2 FTCA, 10:2 FTUCA, isotopically labeled 6:2, 8:2, 10:2 1,2- $^{13}\text{C}_2$ -FTCA and unoxidized compound 6:2, 8:2, 10:2 FTOH from (a) no cell, (b) HepG2 cell and (c) HCT116 cell. (d) and (e) have no target ion chromatographic peak in the FTOH@BUT-16 experiment

Figure. S. Does-dependent formation of 6:2, 8:2, 10:2 FTCA from (a) HepG2 cell and (b) HCT116 cell. Data are presented as mean \pm SD at least three replicate experiments. It was conducted using one-way ANOVA, ** $p=0.0024$, *** $p=0.0002$, **** $p<0.0001$.

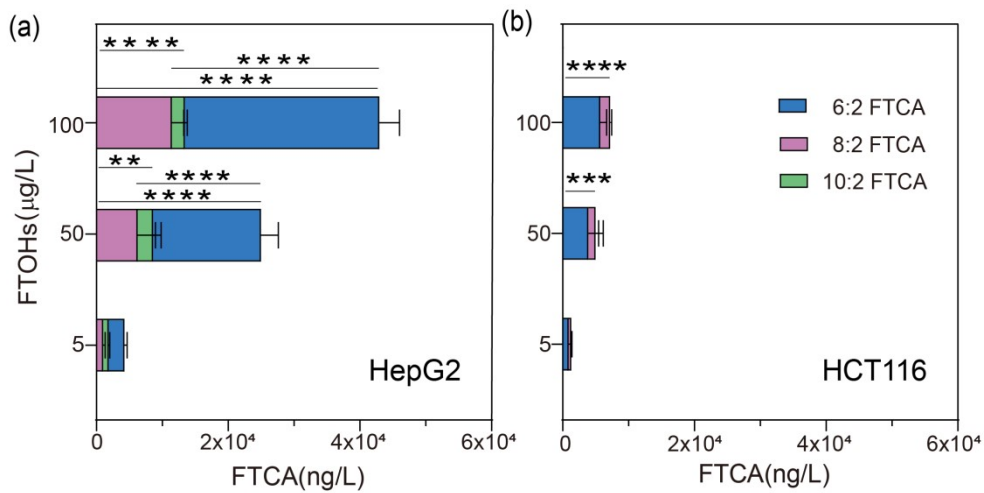


Figure S12. Does-dependent formation of 6:2, 8:2, 10:2 FTCA from (a) HepG2 cell and (b) HCT116 cell. Data are presented as mean \pm SD at least three replicate experiments. It was conducted using one-way ANOVA, ** $p=0.0024$, *** $p=0.0002$, **** $p<0.0001$.

9. Inflammatory cytokine assay

After the cells were treated with FTOHs exposure and FTOH@BUT16 removal, the levels of IL-6 in the supernatant were determined using an ELISA kit (Biorigin (Beijing) Inc., Beijing) according to the manufacturer's instructions. The levels of IL-6 were determined from a standard curve, which was established via a standard substance.

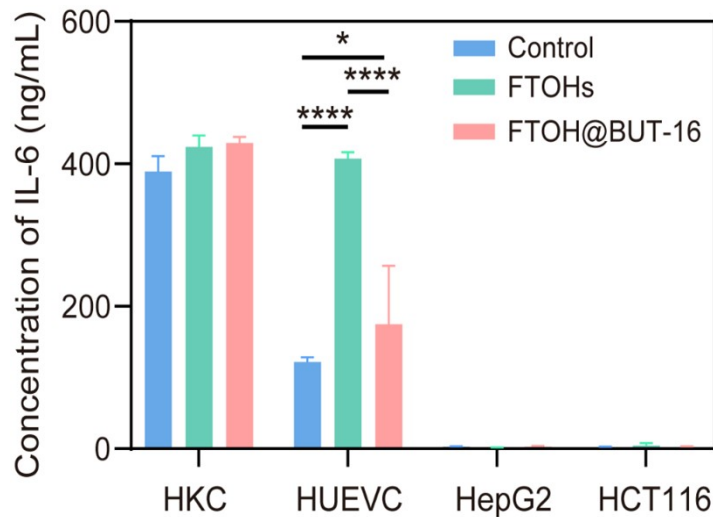


Figure S13. The inflammatory cytokine levels of four types cells in FTOHs exposure and removal groups. Data are presented as mean \pm SD at least three replicate experiments. It was conducted using two-way ANOVA, * $p=0.0418$, **** $p<0.0001$.

Table S1. Parameters of the pseudo-first-order and the pseudo-second order model for the adsorption of FTOHs on BUT-16.

System	Compound	Quasi-primary kinetics			Quasi-secondary kinetics		
		r ²	Q _e (mg/g)	K ₁ (min ⁻¹)	r ²	Q _e (mg/g)	K ₂ (g/(mg·min))
Static adsorption	6:2 FTOH	0.8352	26.9504	0.1213	0.9989	164.2845	0.0109
	8:2 FTOH	0.8144	11.8342	0.1999	0.9999	164.9893	0.0345
	10:2 FTOH	0.7746	11.6697	0.2455	0.9998	166.9728	0.0292
Fluidic adsorption	6:2 FTOH	0.9518	0.6539	0.1231	1	166.6944	0.5749
	8:2 FTOH	0.9554	1.1905	0.1338	1	166.7222	0.3439
	10:2 FTOH	0.9738	0.0660	0.0780	1	166.6667	3.4483

Table S2. Performance of two adsorption systems.

Parameters	Static adsorption	Fluidic adsorption
Adsorption speed	60min	1min
Adsorption efficiency	90%	100%
High throughput	NO	OK
Online adsorption	NO	OK
Security of detoxification	NO	OK

Table S3. Langmuir and Freundlich constants for the sorption of FTOHs using BUT-16.

Compound	Langmuir			Freundlich		
	K _L (L/mg)	Q _m (mg/g)	R ²	K _F ((L/mg) ^{1/n} mg/g)	n	R ²
6:2 FTOH	9.29	321.85	0.9949	224.08	4.36	0.9457
8:2 FTOH	189.04	386.70	0.9872	537.54	4.61	0.9913
10:2 FTOH	522.51	392.77	0.9937	611.55	5.23	0.9804

Table S4. The LOD, calibration, linear ranges and RSD of target compounds.

Compound	LOD ($\mu\text{g/L}$)	R^2	Liner range ($\mu\text{g/L}$)	RSD
6:2 FTOH	1248.57	0.9988	1000-500000	0.0898-9.0516
8:2 FTOH	97.50	0.9701	1000-500000	0.8736-3.9940
10:2 FTOH	56.67	0.9637	1000-500000	0.4609-7.3837
6:2 FTCA	1.53	0.9819	0.1563-10	3.5913-18.9764
8:2 FTCA	1.02	0.9914	0.1563-10	7.6173-23.0938
10:2 FTCA	0.81	0.9814	0.1563-10	2.6220-21.0118

Table S5. A list of 65 metabolites identified with database.

No.	Compound name	t_R	Precursor ion (m/z)	product ion (m/z)	CE (eV)
1	O-Phosphoethanolamine	2.567	142.10	44.20	-13
2	Glucose	2.017	179.20	89.10	8
3	Gluconic acid	2.135	195.20	74.90	17
4	Threonic acid	2.136	135.20	75.00	14
5	Cystine	4.881	241.00	73.90	-29
6	Asparagine	3.068	133.10	28.05	-29
7	Aspartic acid	2.859	134.00	74.05	-15
8	Serine	3.081	105.90	60.10	-12
9	4-Hydroxyproline	2.781	132.10	68.05	-22
10	Sucrose	2.096	341.30	89.05	20
11	Glyceric acid	1.245	105.20	75.10	15
12	Glutamine	3.231	145.20	127.15	14
13	Cysteine	3.120	122.00	76.05	-16
14	Threonine	3.133	120.10	74.15	-13
15	Methionine sulfoxide	3.029	166.00	74.10	-14
16	Glutamic acid	3.199	147.90	84.10	-17
17	Alanine	3.512	89.90	44.10	-12
18	Citrulline	3.668	176.10	70.05	-25
19	Cytidine monophosphate	2.622	324.00	112.05	-14
20	Malic acid	3.402	167.10	123.95	19
21	Ornithine	3.108	133.10	116.05	-15
22	Glucosamine	2.572	180.00	162.10	-12
23	Ascorbic acid	1.605	175.20	87.00	20
24	Proline	3.170	116.10	70.15	-18
25	Lysine	3.210	147.20	130.10	-16
26	Glycyl-glutamine	1.161	132.10	69.15	-19
27	Lactic acid	2.148	89.35	43.00	13
28	2-Aminoadipic acid	3.483	162.15	55.15	-28
29	Uracil	3.653	113.00	70.00	-17
30	Adenosine monophosphate	7.873	348.00	136.05	-20
31	N-Acetylaspartic acid	8.336	175.90	134.05	-12
32	Ethylenediamine	2.352	61.15	44.10	-14
33	5-Oxoproline	2.136	128.20	84.05	12
34	Putrescine	7.087	89.20	72.10	-11
35	Nicotinic acid	4.136	124.05	80.05	-22
36	Choline	9.809	104.10	60.05	-22
37	5-Glutamylcysteine	6.288	169.90	152.05	-15
38	Glutathione	2.331	308.00	179.10	-13
39	Hypoxanthine	4.389	137.00	110.00	-22
40	Valine	4.113	118.00	57.10	-30
41	Uridine	7.945	245.00	113.05	-22

42	Pipecolic acid	3.200	130.10	84.05	-18
43	Methionine	4.335	149.90	56.10	-18
44	Niacinamide	8.626	123.10	80.05	-23
45	N-Acetylcysteine	8.666	164.10	122.10	-14
46	Guanosine	2.346	284.00	152.00	-12
47	Xanthosine	2.393	284.90	153.05	-10
48	Cytidine	8.086	244.10	112.05	-13
49	Thymidine	1.856	243.10	127.10	-12
50	Adenine	4.388	136.00	119.05	-26
51	Pantothenic acid	2.092	220.10	90.15	-15
52	Tyrosine	5.066	182.10	136.10	-15
53	Adenosine	2.244	268.10	136.05	-18
54	Deoxycytidine	1.217	228.10	95.05	-38
55	4-Hydroxyphenyllactic acid	4.808	181.20	135.10	16
56	Pyridoxal	4.336	167.90	150.05	-13
57	Folic acid	10.598	442.00	295.15	-15
58	Riboflavin	2.003	377.00	243.05	-23
59	Isoleucine	6.318	132.10	86.20	-12
60	Biotin	5.382	245.10	226.95	-13
61	Leucine	6.305	132.10	86.05	-12
62	3-Methyl-2-oxovaleric acid	2.612	129.20	85.10	9
63	Tryptophan	13.251	205.10	188.15	-12
64	Penicillin G	10.755	335.10	160.00	-11
65	Ergocalciferol	9.6	397.35	379.30	-12

References

1. D. Qin, Y. Xia and G. M. Whitesides, *Nat. Protoc.*, 2010, **5**, 491-502.
2. B. Wang, P. Wang, L.-H. Xie, R.-B. Lin, J. Lv, J.-R. Li and B. Chen, *Nat. Commun.*, 2019, **10**, 3861.
3. J. H. Cavka, S. Jakobsen, U. Olsbye, N. Guillou, C. Lamberti, S. Bordiga and K. P. Lillerud, *J. Am. Chem. Soc.*, 2008, **130**, 13850-13851.
4. G. Wang, C.-T. He, R. Huang, J. Mao, D. Wang and Y. Li, *J. Am. Chem. Soc.*, 2020, **142**, 19339-19345.
5. M. Y. Zorainy, M. Gar Alalm, S. Kaliaguine and D. C. Boffito, *J. Mater. Chem. A*, 2021, **9**, 22159-22217.
6. K. Zhang, J. Huang, G. Yu, Q. Zhang, S. Deng and B. Wang, *Environ. Sci. Technol.*, 2013, **47**, 6471-6477.